Charge transfer state energy in ternary bulk-heterojuncton polymer-fullerene solar cells

Document status and date:
Published: 01/01/2015

Document Version:
Publisher's PDF, also known as Version of Record (includes final page, issue and volume numbers)

Please check the document version of this publication:

• A submitted manuscript is the version of the article upon submission and before peer-review. There can be important differences between the submitted version and the official published version of record. People interested in the research are advised to contact the author for the final version of the publication, or visit the DOI to the publisher's website.
• The final author version and the galley proof are versions of the publication after peer review.
• The final published version features the final layout of the paper including the volume, issue and page numbers.

Link to publication

Download date: 16. Nov. 2023

Charge transfer state energy in ternary bulk-heterojunction polymer–fullerene solar cells

Sandra Kouijzer
Weiwei Li
Martijn M. Wienk
René A. J. Janssen

SPIE.

Charge transfer state energy in ternary bulk-heterojunction polymer–fullerene solar cells

Sandra Kouijzer, Weiwei Li, Martijn M. Wienk, and René A. J. Janssen*
Eindhoven University of Technology, Institute of Complex Molecular Systems, Molecular
Materials and Nanosystems, PO Box 513, Eindhoven, Netherlands 5600 MB

Abstract. In ternary bulk heterojunction solar cells based on a semiconducting biphenyl-dithie-nyldiketopyrrolopyrrole copolymer donor and two different fullerene acceptors that distinctly differ in electron affinity, the open-circuit voltage is found to depend in a slightly sublinear fashion on the relative ratio of the two fullerenes in the blend. Similar effects have previously been observed and have been attributed to the formation of an alloyed fullerene phase possessing electronic levels that are the weighted average of the two components. By analyzing the contribution of the charge transfer (CT)-state absorption to the external quantum efficiency of the ternary blend solar cells as a function of composition, we find no evidence for a CT state formed between the polymer and an alloyed fullerene phase. Rather, the results are consistent with the presence of two distinct CT states, one for each polymer–fullerene combination. The two-state CT model does not, however, explain the sublinear behavior of the open-circuit voltage as a function of the blend composition. © *2015 Society of Photo-Optical Instrumentation Engineers (SPIE)* [DOI: 10.1117/1.JPE.5.057203]

1 Introduction

In the most efficient bulk heterojunction solar cells, a binary blend of a semiconducting donor polymer and a fullerene acceptor derivative is used as the active layer.[1] Next to binary blends ternary blends are also being considered as photoactive layers.[2–10] The topic attracts interest and has been the subject of several recent reviews.[11–13] There are various reasons why ternary blends can be beneficial as compared to binary blends.

One important reason is extending the absorption spectrum and maintaining a high absorption coefficient. Most conjugated polymers have an intense, but rather narrow absorption band. At higher photon energies above the band gap, the absorption coefficient is often reduced. For small band gap polymer solar cells absorbing in the near-infrared, this leads to a reduced absorption of light in the visible region and an overall lower short-circuit current (J_{sc}). This can be alleviated by using two different conjugated polymer donors that have complementary wide and small band gap absorption spectra in a ternary blend with a fullerene acceptor. With such a combination, it is possible to create a panchromatic absorber layer that efficiently absorbs all photons with energies higher than the lowest optical gap.

A second advantage of using ternary blends is the possibility to adjust the open-circuit voltage (V_{oc}). The open-circuit voltage of any solar cell is determined by the quasi-Fermi levels for electrons and holes. In binary polymer-fullerene blends with Ohmic contacts, the quasi-Fermi levels are limited by the HOMO level of the polymer and the LUMO level of the fullerene. Initially, it has been proposed that in ternary blends, the open-circuit voltage will be limited by the highest HOMO and lowest LUMO of the three components.[2] An intriguing example showing that the actual situation is much more complex has been described by Khlyabich and coworkers.[14] They studied a ternary blend consisting of a semiconducting polymer, poly(3-hexylthiophene) (P3HT), and two

different fullerene derivatives, phenyl-C_{61}-butyric acid methyl ester (PCBM) and indene-C_{60} bisadduct (ICBA) [Fig. 1(a)]. The reduction potentials of these two fullerene derivatives are -1.09 and -1.28 V versus ferrocene/ferrocenium.[15] The difference between the LUMO energy levels causes a difference in the open-circuit voltage. P3HT:PCBM cells have $V_{oc} = 0.605$ V and P3HT:ICBA cells have $V_{oc} = 0.844$ V when blended in a 1:1 polymer:fullerene weight ratio. Surprisingly, Khlyabich et al. established that the open-circuit voltage could be varied gradually over the full range between these two extreme values in a near-linear fashion in ternary P3HT:PCBM:ICBA (weight ratio: $1:1 - x:x$) blends as a function of the weight fraction of ICBA relative to the weight of all fullerenes in the film $\{x = w(\text{ICBA})/[w(\text{PCBM}) + w(\text{ICBA})]\}$. For these ternary blends, the fill factor remained constant (FF = 0.57 to 0.60), while the short-circuit current showed a small but distinct decrease from 9.90 to 8.23 mA/cm^2 going from $x = 0$ to $x = 1$.[14] The remarkable result is that the difference in the reduction potential of $\sim$190 meV between PCBM and ICBA, which amounts to about seven times the thermal energy at room temperature, apparently does not lead to charge trapping at the lower LUMO.

Kang and coworkers, however, observed a different effect.[16] They studied a system of P3HT and an o-xylenyl C_{60} mono-adduct (OXCMA), with either the o-xylenyl C_{60} bisadduct (OXCBA) or the o-xylenyl C_{60} trisadduct (OXCTA) as the ternary component. The LUMO levels estimated by cyclic voltammetry measurements increased for the higher adducts (OXCMA: -3.83 eV, OXCBA: -3.66 eV, and OXCTA: -3.50 eV). As a result, the V_{oc} of the binary blends of these adducts with P3HT increases from 0.634, via 0.834, to 0.899 V. Kang et al. show that low amounts of OXCMA act as a trap in the P3HT: OXCTA blends.[16] The current drops to negligible values and the voltage for these devices is smaller than the voltage of either of the two pure binary blends. For the ternary blend of P3HT, OXCMA, and OXCBA, this trapping does not occur and the V_{oc} increases gradually with composition but more steeply for a lower OXMA concentration. The differences are likely related to the larger offset of the LUMO levels of OXCMA and OXCTA (330 meV) than between OXCMA and OXCBA (170 meV).

Yang et al.[17] investigated two different ternary blends, each with two complementary semiconducting polymer absorbers and PCBM. The external quantum efficiency (EQE) spectrum clearly shows that the photoresponse of these ternary blends has contributions from both polymers. Also, in these ternary blends, the V_{oc} changes gradually when the polymer with the highest
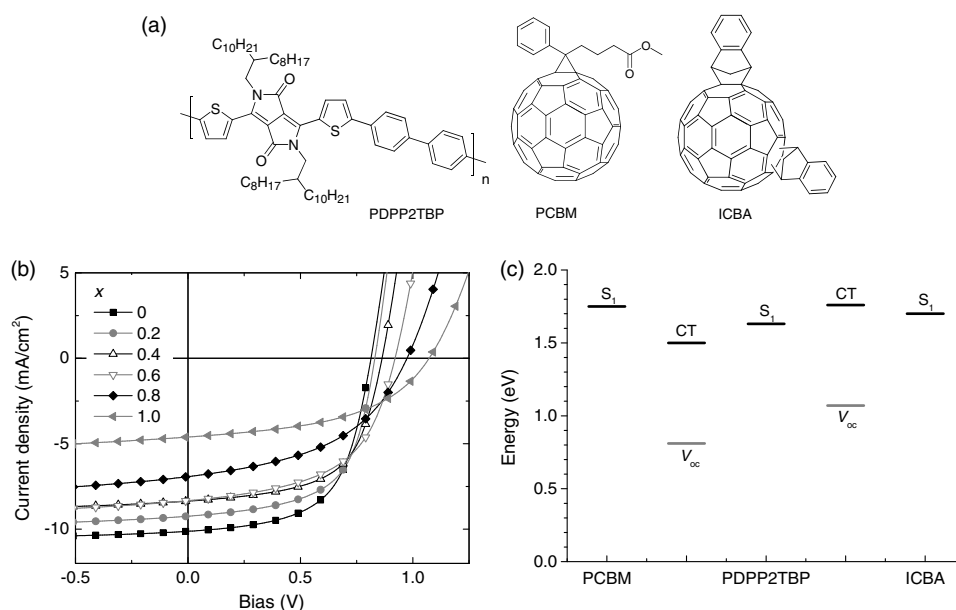

Fig. 1 (a) Structures of PDPP2TBP, phenyl-C_{61}-butyric acid methyl ester (PCBM), and indene-C_{60} bisadduct (ICBA). (b) $J - V$ characteristics of PDPP2TBP:PCBM:ICBA [$1: 2(1 - x): 2x$] solar cells for different compositions x. (c) State energy diagram for PDPP2TBP:PCBM and PDPP2TBP: ICBA blends.

HOMO level is progressively replaced by the polymer with the lower HOMO level. However, there is no increase up to 30% mixing and the increase is much steeper in the later stage when 70 to 100% of the low HOMO polymer is present.

Street et al. investigated the unexpected voltage behavior observed in ternary P3HT:PCBM:ICBA blends in more detail.[18] By performing precise measurements of the EQE as a function of the photon energy, they assessed the states that are able to generate charges. Apart from direct excitation of the donor or acceptor, followed by electron transfer, direct absorption of light into the sub-band gap charge transfer (CT) state is possible. It is well established that the CT state at the interface of the two materials, where the hole is located on the HOMO of the donor and the electron is in the LUMO of the acceptor, can be directly excited, but the absorption coefficient is small. It has also been shown that the CT-state energy is related to the V_{oc}. At room temperature and under one sun illumination intensity, an empirical relation of $qV_{oc} \approx E_{CT} - 0.5$ eV (with q the elementary charge) has been established.[19,20] Street et al. found that the CT-state energy shifts as a function of blend composition (x) in a similar fashion as the open-circuit voltage.[18] More precisely, when measuring the photon energy at a fixed value of the EQE within the broad CT absorption, the value shifts with the PCBM/ICBA ratio in a similar fashion as the change in open-circuit voltage. Street et al. propose that the continuous, almost linear, shift in CT-state energy and in V_{oc} originates from the formation of an alloy between ICBA and PCBM, leading to a mixed acceptor, for which the CT-state energy with P3HT shifts depend on the composition. It is not exactly explained, however, how the alloying can average the LUMO levels of PCBM and ICBA.

To study the possible alloying of PCBM and ICBA in ternary blends, it is of interest to use a polymer with an optical band gap that is better tuned to the solar spectrum than P3HT and that provides a smaller thermalization energy loss ($E_g - qV_{oc}$). In P3HT:PCBM cells, the energy loss from the optical band gap of the polymer ($E_g = 1.9$ eV) and fullerene ($E_g = 1.7$ eV) to qV_{oc} (0.605 eV) is considerable and the spectral coverage is limited to the visible region. Here we use PDPP2TBP, an alternating copolymer of dithienyldiketopyrrolopyrrole (DPP2T) and biphenyl (BP) [Fig. 1(a)].[21] PDPP2TBP has an optical band gap at 1.63 eV and provides solar cells with V_{oc}'s of 0.81 and 1.07 V in combination with PCBM and ICBA, respectively. To study the possible alloying, the EQE of PDPP2TBP:PCBM:ICBA bulk heterojunction solar cells was measured for a range of compositions and fitted to two different models: one for an alloyed CT state and one for a mixture of two CT states. The later model fits the results best.

2 Experimental

PDPP2TBP was synthesized as described previously.[21] PCBM and ICBA were obtained from Sollene BV. Photovoltaic devices were made by spin coating PEDOT:PSS (Hereaus, VP Al4083) onto precleaned, patterned ITO substrates (14 Ω per square) (Naranjo Substrates). The photoactive polymer:fullerene layers were deposited from chloroform using 3% 1-chloronaphthalene (1-CN) as a cosolvent. The back electrode, consisting of LiF (1 nm) and Al (100 nm), was deposited by vacuum evaporation at $\sim 3 \times 10^{-7}$ mbar. The active area of the cells was 0.091 or 0.16 cm^2.

Current density–voltage characteristics were recorded using a Keithley 2400 source meter. White light 100 mW/cm^2 illumination was provided by a tungsten halogen lamp corrected with a Schott GG385 UV filter and a Hoya LB120 daylight filter. EQE measurements were performed with the devices kept in a nitrogen-filled sealed box with a quartz window and illuminated through an aperture of 2 mm. Mechanically modulated (Stanford Research, SR 540) monochromatic (Oriel, Cornerstone 130 Monochromator) light from a 50 W tungsten halogen lamp (Osram 64610) was used as a probe light, in combination with a continuous bias light from a solid-state laser (B&W Tek Inc., 532 nm) to create a representative illumination intensity for 1 sun conditions. The response was amplified with a Stanford Research Systems SR570 low-noise preamplifier and recorded using a lock-in amplifier (Stanford Research Systems SR830).

Transmission electron microscopy (TEM) was performed on a Tecnai G2 Sphera TEM (FEI) operated at 200 kV. Bright-field TEM images were acquired under slight defocusing conditions.

3 Results and Discussion

3.1 *Ternary Blends of PDPP2TBP, PCBM, and ICBA*

PDPP2TBP is a wide band gap analogue of PDPPTPT, which has a single phenyl ring between adjacent thiophene rings instead of biphenyl and reaches a power conversion efficiency of 7.4% in combination with the C_{70} analogue PCBM.[22,23] The addition of the extra phenyl ring into PDPP2TBP increases the optical band gap from 1.53 to 1.63 eV, but the V_{oc} of the solar cell does not change and remains at 0.80 V when mixed with PCBM.[21] The relative large energy loss ($E_g - qV_{oc} = 0.83$ eV) for the PDDP2TBP:PCBM cell suggests that it is possible to achieve a higher V_{oc} when PCBM is replaced by ICBA. Indeed, for PDDP2TBP:ICBA solar cells, V_{oc} increases to 1.07 V [Fig. 1(b)], but the concomitant loss in J_{sc} by more than a factor of two results in an overall lower performance. Hence, by decreasing the thermalization losses ($E_g - qV_{oc}$), the quantum yield for charge separation has decreased. The loss of J_{sc} when replacing PCBM with ICBA is more commonly observed,[15,24,25] but distinct exceptions, such as with P3HT (Ref. 26) and PSPDTTBT (Ref. 27), are known. The loss in J_{sc} is commonly ascribed to a too small offset between the optical band gap E_g and the CT-state energy (E_{CT}),[15,26,27] but also morphological differences can contribute to the loss in J_{sc}.[28] For PDDP2TBP:ICBA, the energy difference $E_g - qV_{oc}$ is reduced to 0.56 eV. This is just below the limit of 0.60 eV that has been proposed by Veldman et al. as being the lower limit for efficient photoinduced charge separation.[20] This explains the loss in J_{sc}. An approximate state diagram of the PDPP2TBP blends with PCBM and ICBA is shown in Fig. 1(c). The energies of the CT states depicted in Fig. 1(c) are discussed in Sec. 3.3. For P3HT:PCBM and P3HT:ICBA cells, the energy losses $E_g - qV_{oc}$ are 1.30 and 1.05 eV, respectively, when compared to the band gap of P3HT and are much larger than the 0.6 eV threshold. This explains why P3HT:ICBA cells can have a high J_{sc}. Alternatively, for PDPPTPT:PCBM blends, the thermalization energy loss ($E_g - qV_{oc} = 1.53 - 0.80 = 0.73$ eV) is already close to the 0.6 eV threshold and the use of ICBA with PDPPTPT will rapidly reduce the quantum efficiency for charge separation.

Inspired by the results of Street et al., we thought it to be of interest to study how J_{sc} and V_{oc} change in ternary blends consisting of PDPP2TBP and PCBM-ICBA mixtures as a function of the PCBM:ICBA ratio but with the total weight ratio of polymer to fullerene constant at the optimized value of 1:2. The solar cells with a device configuration glass/indium tin oxide (ITO)/poly(3,4-ethylenedioxythiophene) poly(styrenesulfonate) (PEDOT:PSS)/PDPP2TBP: PCBM:ICBA [weight ratio: 1: 2(1 − x): 2x]/LiF/Al were made for x increasing from 0 to 1 in steps of 0.1. The resulting current density—voltage ($J - V$) curves are shown in Fig. 1(b) and the corresponding device parameters are collected in Table 1.

The $J - V$ curves show a gradual increase in V_{oc} (0.81 to 1.07 V) and a gradual decrease in J_{sc} (11.02 to 4.61 mA/cm^2) with increasing concentration of ICBA. Also, the FF of the devices drops with an increasing amount of ICBA. The morphology of the PDPP2TBP:PCBM:ICBA blends with 1:2:0, 1:1:1, and 1:0:2 wt.% mixtures studied by bright-field TEM did not show significant differences (Fig. 2). Also, in AFM (not shown), no significant differences were observed. The origin of the gradual increase in V_{oc}, therefore, mainly originates from the changing electronic structure of the blend as a function of composition.

3.2 *CT-State Contribution to EQE*

To study the origin of the change in V_{oc} as a function of PCBM/ICBA ratio, EQE measurements were performed in the spectral range from 350 to 1200 nm. The data depicted in Fig. 3(a) clearly show the contributions of absorption of light by the fullerene in the wavelength ranging between 350 and 500 nm and by the polymer in the high-wavelength regime between 500 and 750 nm. The decrease of J_{sc} with an increasing amount of ICBA is also reflected in the EQE spectrum. The EQE deceases in absolute value over the entire wavelength range. The EQE maximum drops from 0.66 for the PDPP2TBP:PCBM cell to 0.28 for the PDPP2TBP:ICBA cell [Fig. 3(a)].

Figure 3(b) shows the same EQE data, but in a semilogarithmic plot as a function of the photon energy, after normalization of each individual curve to the maximum EQE. In Fig. 3(b), the contribution of the CT-state absorption to the EQE is visible in the region between

Table 1 Device parameters of ternary PDPP2TBP:phenyl-C_{61}-butyric acid methyl ester (PCBM): indene-C_{60} bisadduct (ICBA) [1: 2(1 – x): 2x] bulk heterojunction solar cells for different compositions.

x	J_{sc} (mA/cm^2)	V_{oc} (V)	Fill factor	Power conversion efficiency (%)
0.0	11.02	0.81	0.61	5.41
0.1	10.06	0.82	0.59	4.80
0.2	9.69	0.83	0.60	4.86
0.3	9.48	0.84	0.58	4.63
0.4	8.45	0.86	0.60	4.35
0.5	9.12	0.88	0.56	4.48
0.6	8.30	0.92	0.54	4.15
0.7	7.41	0.94	0.54	3.74
0.8	7.05	0.97	0.47	3.19
0.9	5.41	1.02	0.48	2.67
1.0	4.61	1.07	0.48	2.39
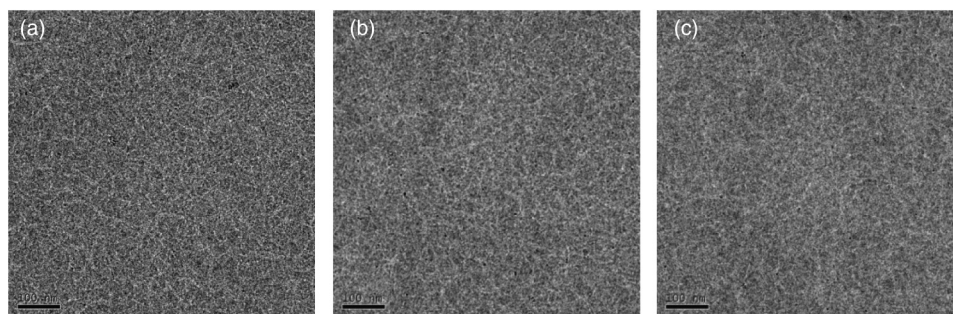
Fig. 2 Bright-field transmission electron microscopy images of blends of PDPP3TBP with PCBM and ICBA. (a) Polymer, poly(3-hexylthiophene) (P3HT):PCBM (1:2). (b) P3HT:PCBM:ICBA (1:1:1). (c) P3HT:ICBA (1:2). The scale bar represents 100 nm.
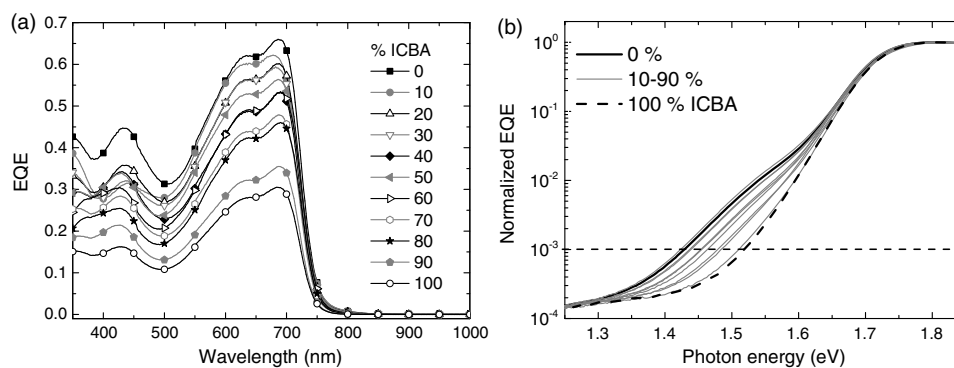
Fig. 3 (a) External quantum efficiency (EQE) versus wavelength of PDPP2TBP:PCBM:ICBA solar cells function of the relative amount of ICBA (x). (b) Normalized EQE as function of photon energy.

1.35 and 1.65 eV (950 to 750 nm), i.e., below the onset of absorption of PDPP2TBP. A clear trend is visible. The low-energy shoulder in the graph disappears when PCPM is replaced by ICBA, which suggests that the CT-state contribution shifts to higher energies for solar cells with more ICBA.

Figure 4 directly compares the shift in the CT band with the shift in V_{oc} as function of the ICBA content. The energy of the CT band was arbitrarily taken as the photon energy, where the normalized EQE has dropped to a value of 10^{-3} of its maximum [dashed line in Fig. 3(b)]. Figure 4 shows that there is a distinct difference in the shift of V_{oc} and the shift of CT-state energy. The change in V_{oc} is ∼0.26 V, but the change in CT energy is only 0.10 eV and is only about half of the 0.19 eV difference between the reduction potentials of PCBM and ICBA.

3.3 Modeling of EQE

To understand the origin of the changes in the EQE data as a function of composition, the data are modeled in two different ways. First, an alloy CT-state model, where the PCBM:ICBA clusters are thought to be present, which have a reduction potential that depends on the weighted cluster composition such that the CT-state energy shifts linearly with composition. This alloy CT-state model is inspired by the work of Street et al.[18] The second is a two CT-state model, which assumes that two distinct CT states are present, one for PDPP2TBP:PCBM and one for PDPP2TBP:ICBA, whose relative contributions depend on the PCBM:ICBA ratio in the ternary blend. Since the difference in voltage between the solar cells with pure fullerenes is 0.26 V, the CT state is assumed to shift over or differ by 0.26 eV depending on the model used. To validate both models, the EQE spectra of the intermediate blends are calculated and compared with the experimental EQE data.

The first step in making a quantitative model is to determine the location of the maximum photon energy of the CT band from the EQE. To this end, the normalized EQE curve of the PDPP2TBP:ICBA blend is subtracted from the normalized PDPP2TBP:PCBM EQE curve. This results in the red curve shown in Fig. 5, of which the low-energy branch resembles a Gaussian function. Based on Marcus electron transfer theory,[29,30] Vandewal et al. showed that the following relation applies for the EQE in the spectral range of the CT-state absorption as function of the photon energy E:[31]

$$\text{EQE}_{\text{CT}}(E) = \frac{f}{E\sqrt{4\pi\lambda kT}}\exp\left[-\frac{(E_{\text{CT}} + \lambda - E)^2}{4\pi\lambda kT}\right], \tag{1}$$

where λ is the reorganization energy, k is the Boltzmann constant, T is the absolute temperature, and f is a parameter proportional to the coupling matrix element squared and further includes the thickness of the layer and internal quantum efficiency. Fitting Eq. (1) to the difference EQE spectrum gives $E_{\text{CT}} = 1.50$ eV and $\lambda = 0.22$ eV, such that the maximum of the CT band
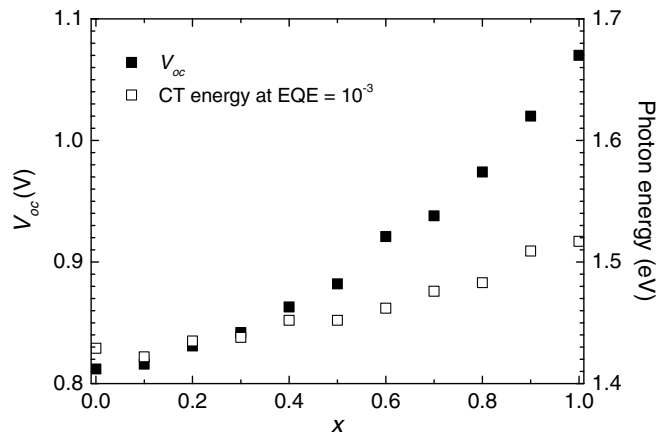

Fig. 4 V_{oc} and photon energy at a normalized EQE $= 10^{-3}$ for PDPP2TBP:PCBM:ICBA solar cells as function of the relative amount of ICBA (x).
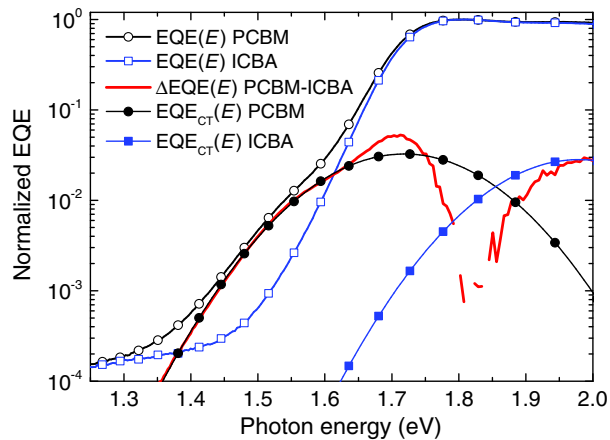
Fig. 5 Determination of the charge-transfer (CT) state absorption spectra of PDPP2TBP:PCBM and PDPP2TBP:ICBA blends. The former is determined by subtracting the EQE spectra of the two cells (red curve) and fitting this to Eq. (1) for EQECT(E) (black markers). The latter is obtained by shifting the first over 0.26 eV over the photon energy axis.

$(E_{CT} + \lambda)$ is found at 1.72 eV (Fig. 5). The value for λ falls within the range of $\lambda = 0.2$ to 0.3 eV, which is commonly observed for polymer–fullerene blends.[32] The value of $E_{CT} = 1.50$ eV is higher than expected when compared to the empirical relation $E_{CT} = qV_{oc} + 0.5$ eV, which would place $E_{CT} \approx 1.30$ eV.[19,20] However, as Vandewal et al. have pointed out,[32] this difference relates to the different definition of E_{CT} in Eq. (1) as compared to the definition used in the empirical relation in previous publications.[19,20,33] The difference has been estimated to be ~0.2 eV,[32] which reconciles the seeming discrepancy.

Now that the CT-state absorption of PDPP2TBP:PCBM is known, the CT-state absorption of PDPP2TBP:ICBA can be estimated by adding the V_{oc} difference (0.26 V), resulting in $E_{CT} = 1.76$ eV. Both the shape and height of the CT absorption band of PDPP2TBP:ICBA are assumed to be identical to those of PDPP2TBP:PCBM. We note that $E_{CT} - qV_{oc}$ is not a constant and may vary by ±0.1 eV for different materials. The lower photocurrent and FF found in PDPP2TBP:ICBA blends suggest that bimolecular recombination is more pronounced than in PDPP2TBP:PCBM cells. In such a case, $E_{CT} - qV_{oc}$ would be larger and, hence, the value of $E_{CT} = 1.76$ eV would be a lower estimate.

The estimated CT-state energy of $E_{CT} = 1.76$ eV is significantly above the optical band gap of PDPP2TBP ($E_g = 1.63$ eV). Hence, the contribution of the weak CT absorption to the EQE spectrum of PDPP2TBP:ICBA will be masked by the much stronger direct absorption of PDPP2TBP. In addition, $E_{CT} = 1.76$ eV is also larger than the energy of the lowest singlet excited state (S_1) of ICBA at 1.70 eV [Fig. 1(c)], which can be inferred from the 0-0 vibronic peak of the photoluminescence of ICBA in thin films.[15] The fact that the CT state in PDPP2TBP:ICBA blends is slightly above the singlet-state energies of both components explains the loss in J_{sc} for these blends compared to PDPP2TBP:PCBM blends, where the CT state is lower [Fig. 1(c)].

For the alloy CT-state model, the CT-state absorption band shifts in small steps to a higher energy. The step size is the fraction of ICBA relative to PCBM + ICBA multiplied by the total energy difference of 0.26 eV. This energy-shifted EQE in the spectral range of the CT is subsequently added to the EQE data of PDPP2TBP:ICBA to obtain the EQE for the alloying model [Fig. 6(a)]. A similar approach is used for the two CT-state model. Here, the intensities of the CT-absorption bands of PDPP2TBP:PCBM and PDPP2TBP:ICBA are multiplied with their relative concentrations. Both weighted CT-state contributions to the EQE are added to the experimental EQE data for PDPP2TBP:ICBA to obtain the modeled EQE curves for each different fraction [Fig. 6(b)]. The resulting modeled EQE curves for the alloy CT-state model and the two CT-state model are shown in Fig. 6.

To compare both models to the experimental EQE data, the photon energy where the normalized EQE reaches 10^{-3} is plotted in Fig. 7. Figure 7 demonstrates a much better correspondence of the two CT-state model to the experiment than the alloy CT-state model. For the alloy CT model, the shift in CT-state energy remains constant for ICBA percentages >60%. This
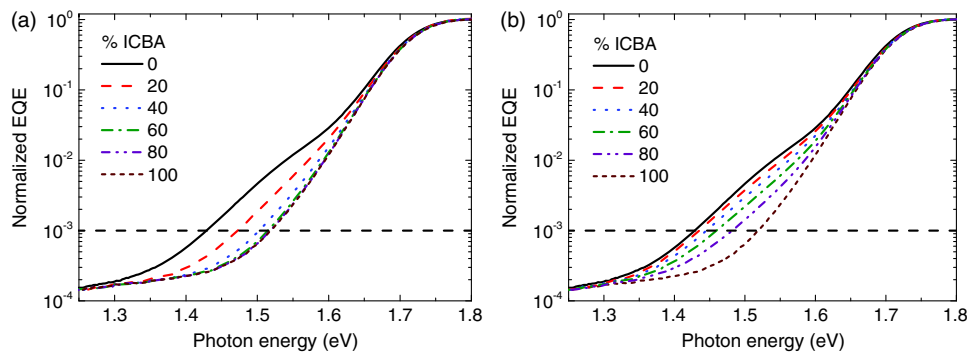
Fig. 6 Modeled EQE curves for different relative amounts of ICBA (x). (a) The alloy CT-state model. (b) The two CT-state model. The photon energies where the dashed line at EQE = 10^{-3} intersects with the EQE data are plotted in Fig. 7.
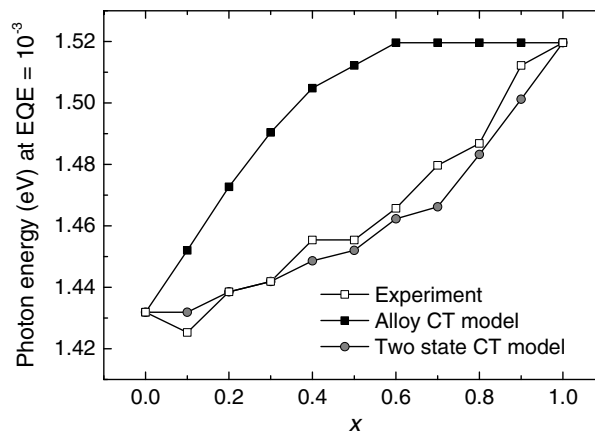

Fig. 7 Photon energy at a normalized EQE = 10^{-3} for ternary PDPP2TBP:PCBM:ICBA solar cells as function of the relative amount of ICBA (x). The experimental data (open squares) are compared to two models: the alloy CT-state model (solid squares) and the two CT-state model (solid circles).

relates to the fact that the EQE from the shifting CT band becomes completely obscured by the much more intense EQE arising from excitation of the polymer. On the other hand, the two CT-state model accurately describes both the shape and the magnitude of the measured data of the onset of the EQE versus ICBA content.

Because the DPP2TBP:ICBA CT band cannot be observed directly, there is some ambiguity on the exact shape, height, and position of this band. However, the quality of the correspondence between the experiment and the two CT-state model is striking, despite the fact that we use the most straightforward approximation. We note that the changes in the low-energy region of the EQE spectra with composition are largely dominated by the disappearance of the PDPP2TBP:PCBM CT band (Fig. 5). The grow-in of the PDPP2TBP:ICBA CT band has a small effect because it is largely hidden under the absorption tail of PDPP2TBP (Fig. 5).

From this modeling, it can be concluded that alloying of the fullerenes does not accurately describe the changes in the EQE spectra with composition, and hence, the analysis of the EQE strongly favors an understanding in terms of two distinct CT states that both contribute to the EQE at low photon energies.

3.4 Modeling the J – V Curves

Although the EQE data are satisfactorily described by the two CT-state model, this model does not really answer the question of why the V_{oc} changes gradually. Because the LUMO level of PCBM is 0.19 eV lower than that of ICBA, the former would actually be expected to pin the V_{oc} to the LUMO level of PCBM for most blends. One possibility is the presence of a parallel tandem
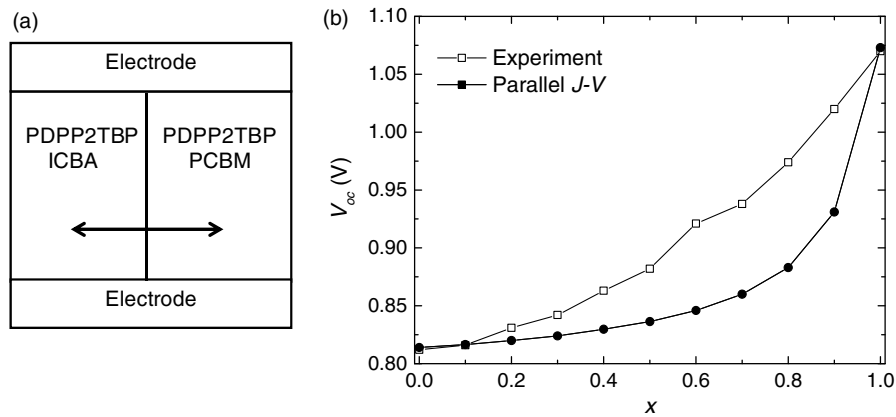
Fig. 8 (a) Schematic representation of the parallel ternary bulk heterojunction. (b) Shift in V_{oc} for the experimental and parallel tandem model.

junction in the device on a nanoscale. This configuration has been termed as a parallel bulk heterojunction cell in the literature.[17] To understand its operation, it is useful to consider a parallel tandem cell. In a parallel tandem connection, the voltage over the two subcells is necessarily the same and is mainly determined by the subcell with the lowest band gap.[34,35] The currents through the two subcells can differ. In a parallel bulk heterojunction cell,[17] two subcells are thought to be present in one bulk heterojunction blend as schematically depicted in Fig. 8(a). Excitons are separated into charges in two spatially different (nanoscale) regions. In the present example, this would be a PDPP2TBP:PCBM region and a PDPP2TBP:ICBA region. This model is also consistent with the two CT-state model inferred from the EQE analysis. Depending on the relative domain sizes of the two regions, one can expect the voltage to change, although it is likely that it will be dominated by the voltage of the PDPP2TBP:PCBM regions.

To test this explanation, the $J - V$ curves of the ternary P3HT:PCBM:ICBA blend were modeled as a parallel bulk heterojunction empirically. The morphology of the photoactive layer is assumed to mimic a parallel tandem cell. Hence, at each voltage, the current density of the subcells can be added to obtain the $J - V$ curve of the parallel junction. A linear combination of the $J - V$ curves of the individual subcells is taken to calculate the $J - V$ curves of the different blends using $J(V) = (1 - x)J_{PCBM}(V) + xJ_{ICBA}(V)$. Before adding the $J - V$ curves, they were first corrected for the series resistance of the cell caused by the series resistance of the ITO contact ($R_s = 25\ \Omega$), using $V_{corr} = V - JR_s$. The open-circuit voltages resulting from adding the corrected $J - V$ curves are shown in Fig. 8(b) (solid squares). When the modeled V_{oc} is compared to the experimental V_{oc} as a function of x, it can clearly be seen that the modeled V_{oc} is significantly more sublinear than the measured V_{oc}. Hence, this parallel tandem configuration does not explain the gradual sublinear dependence of V_{oc} found experimentally, and hence, such an explanation needs further study.

4 Conclusion

We have studied the origin of the V_{oc} in ternary PDPP2TBP:PCBM:ICBA bulk heterojunction blend solar cells. Similar to previous results published for ternary P3HT:PCBM:ICBA blends,[14,18] the V_{oc} is found to shift gradually and is slightly sublinear with the relative concentration of PCBM and ICBA over a range as large as 0.26 V. The remarkable result is that the V_{oc} is not pinned by the LUMO level of PCBM, which is 0.19 eV lower in energy than the LUMO of ICBA.

In search for the origin of this gradual shift, we measured the contribution of the CT-state absorption to the EQE. The changes in the EQE in the spectral range of the CT-state absorption were simulated using two different models as a function of the composition. The first model assumes that a single CT-state energy exists at the interface of PDPP2TBP with PCBM:ICBA alloy clusters.[18] The second model assumes that PDPP2TBP forms distinct CT states

with PCBM and ICBA. The modeling results show that the latter two CT-state model fits the experimental results, whereas the former, the alloy CT-state, model does not.

In an attempt to explain the gradual shift in CT-state energy, the ternary PDPP2TBP:PCBM:ICBA blends were modeled as a so-called parallel tandem bulk heterojunction.[17] Combining the $J - V$ characteristics of the two individual cells to simulate a parallel tandem configuration provides a sublinear dependence of the V_{oc} on the blend composition. However, the sublinearity is substantially larger than in the experiment.

In conclusion, the EQE results suggest that it is unlikely that an electronically alloyed PCBM: ICBA phase exists in ternary PDPP2TBP:PCBM:ICBA blends. The EQE data can only be explained with two distinct CT states that both contribute to the absorption of light, depending on the relative concentration of the two fullerene acceptors. The mechanism that gives rise to the slightly sublinear dependence of the V_{oc} on blend composition remains to be explained.

Acknowledgments

References

1. Z. He et al., "Enhanced power-conversion efficiency in polymer solar cells using an inverted device structure," *Nat. Photonics* **6**, 591–595 (2012).
2. M. Koppe et al., "Near IR sensitization of organic bulk heterojunction solar cells: towards optimization of the spectral response of organic solar cells," *Adv. Funct. Mater.* **20**, 338–346 (2010).
3. T. Ameri et al., "Performance enhancement of the P3HT/PCBM solar cells through NIR sensitization using a small-bandgap polymer," *Adv. Energy Mater.* **2**, 1198–1202 (2012).
4. H. C. Hesse et al., "Perylene sensitization of fullerenes for improved performance in organic photovoltaics," *Adv. Energy Mater.* **1**, 861–869 (2011).
5. Z. Hu et al., "Near-infrared photoresponse sensitization of solvent additive processed poly(3-hexylthiophene)/fullerene solar cells by a low band gap polymer," *Appl. Phys. Lett.* **101**, 053308 (2012).
6. H. Kim, M. Shin, and Y. Kim, "Distinct annealing temperature in polymer:fullerene:polymer ternary blend solar cells," *J. Phys. Chem. C* **113**, 1620–1623 (2009).
7. G. Adam et al., "Mobility and photovoltaic performance studies on polymer blends: effects of side chains volume fraction," *J. Mater. Chem.* **21**, 2594–2600 (2011).
8. M. C. Chen et al., "Improving the efficiency of organic solar cell with a novel ambipolar polymer to form ternary cascade structure," *Sol. Energy Mater. Sol. Cells* **95**, 2621–2627 (2011).
9. S. S. Sharma, G. D. Sharma, and J. A. Mikroyannidis, "Improved power conversion efficiency of bulk heterojunction poly(3-hexylthiophene):PCBM photovoltaic devices using small molecule additive," *Sol. Energy Mater. Sol. Cells* **95**, 1219–1223 (2011).
10. J. M. Lobez et al., "Improving the performance of P3HT–fullerene solar cells with side-chain-functionalized poly(thiophene) additives: a new paradigm for polymer design," *ACS Nano* **6**, 3044–3056 (2012).
11. T. Ameri et al., "Organic ternary solar cells: a review," *Adv. Mater.* **25**, 4245–4266 (2013).
12. L. Yang, L. Yan, and W. You, "Organic solar cells beyond one pair of donor–acceptor: ternary blends and more," *J. Phys. Chem. Lett.* **4**, 1802–1810 (2013).
13. F. Goubard and G. Wantz, "Ternary blends for polymer bulk heterojunction solar cells," *Polym. Int.* **63**, 1362–1367 (2014).

14. P. P. Khlyabich, B. Burkhart, and B. C. Thompson, "Efficient ternary blend bulk hetero-junction solar cells with tunable open-circuit voltage," *J. Am. Chem. Soc.* **133**, 14534–14537 (2011).

15. D. Di Nuzzo et al., "Simultaneous open-circuit voltage enhancement and short-circuit current loss in polymer: fullerene solar cells correlated by reduced quantum efficiency for photoinduced electron transfer," *Adv. Energy Mater.* **3**, 85–94 (2013).

16. H. Kang et al., "Effect of fullerene tris-adducts on the photovoltaic performance of P3HT: fullerene ternary blends," *ACS Appl. Mater. Interfaces* **5**, 4401–4408 (2013).

17. L. Yang et al., "Parallel-like bulk heterojunction polymer solar cells," *J. Am. Chem. Soc.* **134**, 5432–3435 (2012).

18. R. A. Street et al., "Origin of the tunable open-circuit voltage in ternary blend bulk hetero-junction organic solar cells," *J. Am. Chem. Soc.* **135**, 986–989 (2013).

19. K. Vandewal et al., "The relation between open-circuit voltage and the onset of photocurrent generation by charge-transfer absorption in polymer : fullerene bulk heterojunction solar cells," *Adv. Funct. Mater.* **18**, 2064–2070 (2008).

20. D. Veldman, S. C. J. Meskers, and R. A. J. Janssen, "The energy of charge-transfer states in electron donor–acceptor blends: insight into the energy losses in organic solar cells," *Adv. Funct. Mater.* **19**, 1939–1948 (2009).

21. W. W. Li et al., "Wide band gap diketopyrrolopyrrole-based conjugated polymers incorpo-rating biphenyl units applied in polymer solar cells," *Chem. Commun.* **50**, 679–681 (2014).

22. J. C. Bijleveld et al., "Poly(diketopyrrolopyrrole–terthiophene) for ambipolar logic and photovoltaics," *J. Am. Chem. Soc.* **131**, 16616–16617 (2009).

23. K. H. Hendriks et al., "High-molecular-weight regular alternating diketopyrrolopyrrole-based terpolymers for efficient organic solar cells," *Angew. Chem. Int. Ed.* **52**, 8341–8344 (2013).

24. T. E. Kang et al., "Photoinduced charge transfer in donor-acceptor (DA) copolymer: ful-lerene bis-adduct polymer solar cells," *ACS Appl. Mater. Interfaces* **5**, 861–868 (2013).

25. E. T. Hoke et al., "Recombination in polymer:fullerene solar cells with open-circuit voltages approaching and exceeding 1.0 V," *Adv. Energy Mater.* **3**, 220–230 (2013).

26. Y. He et al., "Indene–C60 bisadduct: a new acceptor for high-performance polymer solar cells," *J. Am. Chem. Soc.* **132**, 1377–1382 (2010).

27. J.-H Huang et al., "The investigation of donor-acceptor compatibility in bulk-heterojunction polymer systems," *Appl. Phys. Lett.* **103**, 043304 (2013).

28. S. Shoaee et al., "Charge photogeneration for a series of thiazolo-thiazole donor polymers blended with the fullerene electron acceptors PCBM and ICBA," *Adv. Funct. Mater.* **23**, 3286–3298 (2013).

29. R. A. Marcus, "Relation between charge transfer absorption and fluorescence spectra and the inverted region," *J. Phys. Chem.* **93**, 3078–3086 (1989).

30. I. R. Gould et al., "Radiative and nonradiative electron transfer in contact radical-ion pairs," *Chem. Phys.* **176**, 439–456 (1993).

31. K. Vandewal et al., "Charge-transfer states and upper limit of the open-circuit voltage in polymer:fullerene organic solar cells," *IEEE J. Sel. Topics Quantum Electron.* **16**, 1676–1684 (2010).

32. K. Vandewal et al., "Relating the open-circuit voltage to interface molecular properties of donor:acceptor bulk heterojunction solar cells," *Phys. Rev. B* **81**, 125204 (2010).

33. D. Veldman et al., "Compositional and electric field dependence of the dissociation of charge transfer excitons in alternating polyfluorene copolymer/fullerene blends," *J. Am. Chem. Soc.* **130**, 7721–7735 (2008).

34. T. Ameri, N. Li, and C. J. Brabec, "Highly efficient organic tandem solar cells: a follow up review," *Energy Environ. Sci.* **6**, 2390–2413 (2013).

35. S. Sista et al., "High-efficiency polymer tandem solar cells with three-terminal structure," *Adv. Mater.* **22**, E77–E80 (2010).

Biographies of the authors are not available.